Regular article

PHYSICAL CHEMISTRY RESEARCH
Published by the
Iranian Chemical Society
www.physchemres.org
info@physchemres.org

***Phys. Chem. Res.**, Vol. 1, No. 1, 61-68, June 2013.*

Diffusive Dynamics of Binary Lennard-Jones Liquid in the Presence of Gold Nanoparticle: A Mode Coupling Theory Analysis

L. Separdar and S. Davatolhagh*

Department of Physics, College of Sciences, Shiraz University, Shiraz 71454, Iran

(Received 24 October 2012, Accepted 28 January 2013)

Molecular dynamics simulation has been performed to analyze the effect of the presence of gold nanoparticle on dynamics of Kob-Anderson binary Lennard-Jones mixture upon supercooling within the framework of the mode coupling theory of the dynamic glass transition. The presence of gold nanoparticle has a direct effect on the liquid structure and causes the peaks of the radial distribution functions to become shorter with respect to the bulk binary Lennard-Jones liquid. It is found that the dynamics of the liquid at a given density is consistent with the mode coupling theory (MCT) predictions. In accordance with the idealized MCT, the diffusion constants $D(T)$ show power-law behavior at low temperatures for both types of binary Lennard-Jones (BLJ) particles as well as the 13 gold atoms comprising the nanoparticle. The mode coupling crossover temperature T_c is the same for all particle types, however, $T_c = 0.4$ is reduced with respect to that of the bulk BLJ liquid and the exponent is found to depend on the particle type. The existence of the nanoparticle causes the short-time β-relaxation regime to shorten and the range of validity of the MCT shrink with respect to the bulk BLJ. It is also found that the behavior of intermediate scattering function (ISF) is in agreement with MCT prediction and in spite of the presence of gold nanoparticle the time temperature superposition principle at intermediate and low temperatures is still valid and the curves of ISF *vs.* $t/\tau(T)$ fall onto a master curve.

Keywords: Molecular dynamics simulation, Mode coupling theory, Glass transition, Nanofiller

INTRODUCTION

During the last couple of decades the problem of glass and glass transition has been a matter of considerable interest both theoretically and numerically. Different theories have been proposed for describing the static as well as the dynamic behavior of the supercooled liquids. The mode coupling theory [1], the dynamic heterogeneity [2], the theory of random first-order transition [3], the landscape viewpoint [4] and the theory of frustration limited domains [5], are examples of theories used to describe the behavior of systems in the supercooled regime. The mode coupling theory (MCT) is a theoretical tool for investigating the dynamic behavior of lightly supercooled liquids near their melting point, *i.e.* well above the laboratory glass transition temperature T_g. According to this theory the knowledge of the static structure of the system is sufficient to predict the dynamic evolution of time correlation functions. In its ideal form, where cooperative hopping is neglected, this theory predicts a transition from ergodic to nonergodic state at a temperature T_c (below the melting point but well above the laboratory glass transition T_g). The extensive work done based on the MCT, allows us to identify and understand the subtle path to formation of glasses. Kob and Anderson have discussed in detail the unusual features of binary Lennard-Jones (BLJ) upon supercooling [6] within the framework of the MCT of dynamic glass transition both in the direct and the reciprocal space. More recently, Gallo *et al.* investigated the MCT predictions for the BLJ confined by nanoscale spheres both in the direct- and the Q-space [7]. In this work we attempt to explore how accurate are the predictions of MCT for the BLJ fluid in the presence of a nanoparticle such as gold that is free to move through. The motivation comes from the increasing utility of nanoparticles in glassy materials and the need for understanding the physics of such systems at the molecular level. In fact as the filler size enters the nano-region, the increasing interface area of the liquid and nanofillers, becomes the basis for tremendous changes in the nanocomposite properties. For example in [8] the presence of gold nanoparticle in polymer polyoctylthiophene alters the

*Corresponding author. E-mail: davatolhagh@susc.ac.ir

morphological and spectral features of the polymer. Furthermore, the effect of nanoparticle on dynamics and structure of supercooled liquids is studied *via* simulation and x-ray photon correlation spectroscopy [9,10]. In [11], the silicate nanoparticle is found to significantly affect the diffusion of the polymer, and the high surface of the silica raises the effective glass transition temperature of the polymer matrix in [12].

In this work we investigate, by means of molecular dynamics simulations, the effect of gold nanoparticle on structure and dynamics of the most studied model of glass forming liquids, *i.e.* the Kob-Andeson binary Lennard-Jones fluid, within the framework of the mode coupling theory both in the direct space and wave-vector space. The rest of this paper is organized as follows. In section II the main predictions of the mode coupling theory relevant to our work are briefly reviewed. In section III, we introduce the model system and describe the simulation methodology. In Section IV, the simulation results for the dynamic properties of the system are presented and compared with those of the bulk BLJ. The paper is concluded with a discussion and summary in section V.

MODE COUPLING THEORY

The idealized MCT provides an equation of motion for the time correlation functions, which uses static correlations and interaction potentials as the input. In a temperature range above T_c where the activated hopping processes can be neglected, and below an onset temperature T_{on} where the slow dynamics regime sets in [13], the MCT fares quite well to describe a host of experimental and numerical results. One of the main predictions of MCT within this regime is that the translational diffusion has a power law dependence on temperature:

$$D \sim (T - T_c)^{\gamma} \tag{1}$$

If the correlator of the Fourier components of the particle density fluctuations $\rho_q(t)$ is defined as

$$F(q,t) = \langle \rho_{-q}(0)\, \rho_q(t) \rangle / N \tag{2}$$

then MCT derives the equation of motion for this density correlator. Here $F(q,t)$ is called the intermediate scattering function. This function at $t = 0$ is equivalent to static structure factor. This theory has certain predictions for time evolution of density correlators, if small parameter of the theory $\varepsilon = (T - T_c)/T_c$ tends to zero. The intermediate scattering function in normal liquid exhibits exponential decay, however, in supercooled liquid such simple decay cannot be seen and it changes to stretched exponential decay. This stretched exponential decay can be fitted well by the Kohlrausch-Williams-Watts (KWW) analytical function

$$F(q,t) = f_q e^{-(\frac{t}{\tau})^{\beta}} \tag{3}$$

where β is the Kohlrausch exponent.

In its ideal version, the MCT also predicts that the curves of dynamic properties such as correlation functions for different temperatures *vs*. reduced time, *i.e.* $t/\tau(T)$, where $\tau(T)$ is the associated relaxation time at temperature *T,* fall onto a master curve. This specific α-relaxation scaling law is also called the time-temperature superposition principle:

$$\varphi(t,T) = F(\frac{t}{\tau(T)}) \tag{4}$$

Where $F(t/\tau(T))$ is a master curve that in the late α-relaxation limit becomes the KWW function (3) that the correlation functions $\varphi(t)$ for different temperatures fall onto. In the late β-relaxation and early α relaxation regime, MCT predicts this master curve can be fitted well by

$$F(\frac{t}{\tau(T)}, q) = f_q^c - h_q(\frac{t}{\tau})^b \tag{5}$$

This equation is called von-Schweidler law and τ indicates the characteristic time of relaxation. f_q^c is called the critical non-ergodicity parameter and h_q is a positive factor. These predictions are valid only when hopping processes can be neglected, otherwise they need certain modifications [14-16].

SYSTEM DESCRIPTION AND SIMULATION METHODOLOGY

The system studied in this work, abbreviated by

BLJ+Gold, consists of a gold nanoparticle composed of 13 gold atoms (called C particles) in a liquid $A_{80}B_{20}$ Lennard-Jones binary mixture. The liquid is composed of 800 particles of type A and 200 particles of type B with masses $m_A = m_B = 1$. The mass of gold nanoparticle is 64 m_A. All particles are placed inside a cubic box with an edge length $L = 9.486\sigma_A$, in constant volume. The range of temperatures simulated is $0.4 \leq T \leq 4.0$. Periodic boundary conditions were applied. The interaction potential between the three particle types is that of the Lennard-Jones potential

$$V(r) = 4\varepsilon\mu\nu[(\frac{\sigma\mu\nu}{r})^{12} - (\frac{\sigma\mu\nu}{r})^{6}] \quad (6)$$

where indices μ and ν run on the particle types A, B and C. The values of the parameters for A and B particles are those of Kob-Anderson BLJ liquid. The parameters of interactions between the BLJ particles and the C particles are obtained from the Lorentz-Berthelot combination rules. All potential parameters for different pair interactions are listed in Table 1.

In the following all the results will be given in the usual BLJ units such that length is measured in unit of σ_A, energy in unit of ε_A, and time in unit of $\sqrt{m\sigma_A^2/48\varepsilon_A}$. The temperature unit is ε_A/k_B where k_B is the Boltzmann constant. The integration time step used is 0.002 BLJ unit. The simulations were started at the highest temperature $T = 4$ where the relaxation time is short. Then the temperature of the system was reduced stepwise by coupling it to a Nosé-Hoover thermostat. For every temperature, the final equilibrium state of the system at the adjacent higher temperature was used as the initial configuration. The temperatures studied correspond to $T = 4, 3, 2.5, 2, 1.5, 1, 0.8, 0.7, 0.6, 0.55, 0.5, 0.47, 0.45, 0.42$ and 0.4.

Table 1. The Mutual Interaction Parameters Between A, B and C Particles in BLJ Units

Atom pair	σ	ε
A-A	1	1
A-B	0.80	1.5
B-B	0.88	0.5
C-C	0.77	22.18
A-C	0.885	4.814
B-C	0.825	3.33

RESULTS

In this section the results of the simulations are presented. In the first part we report the dynamic properties of the system in the direct space, and in the second part the dynamics of the system will be investigated in the wave-vector space.

Dynamics in Direct Space

To begin, in Fig. 1 the radial distribution functions for AA, AB and CA pairs for the entire temperature range $0.4 \leq T \leq 4.0$ are plotted. In the figure, the curves for different temperatures are shifted vertically by 0.1n (n = 1, 2, 3, ...) for clarity. In Figs. 1a and b, the second peaks of $g_{AA}(r)$ and $g_{AB}(r)$ start splitting at $T_{on} \approx 0.7$ that also corresponds to the onset of slow dynamics, and indicates that the system is entering the supercooled phase. Figure 1c represents $g_{CA}(r)$ or the static correlation between majority A particles with the gold nanoparticle. By decreasing the temperature we note the gradual enhancement of the first peak of $g_{CA}(r)$. Thus, the structure of the mixture is such that the A particles tend to form a layer around the nanoparticle due to the strong attraction between A and C atoms (see, Table 1).

Figure 2a shows the log-log plot of the mean squared displacement (MSD) $<r^2(t)>$ of A particles versus time for the entire temperature range investigated. For short times, the MSDs are proportional to t^2. This regime corresponds to the ballistic motion. At the onset of the diffusive motion, the MSDs become proportional to t. At high temperatures the ballistic motion goes over immediately into a diffusive motion but for temperatures below the onset of slow dynamics $T_{on} \approx 0.7$, the MSDs do not immediately switch to diffusive regime after the ballistic one, and a plateau appears at intermediate times due to the cage effect of the neighboring coordination shells shown in Fig. 1. This plateau indicates that the system is approaching a glass transition. We note that the dynamic crossover temperature $T_{on} \approx 0.7$ at which a plateau begins to appear, also corresponds to the temperature at which the second peaks in radial distribution functions begin to split, which is indicative of the extended local order that starts to develop in the liquid. From the height of the plateau, one can estimate the cage radius. The value obtained for both A and B

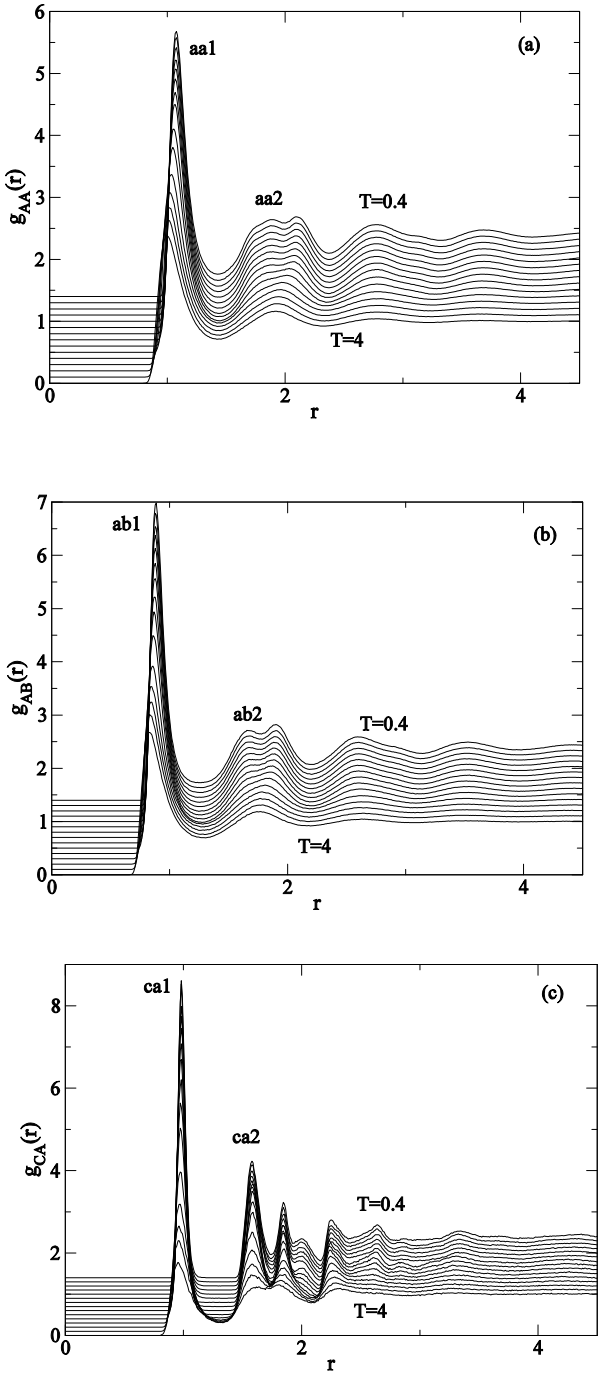

Fig. 1. The radial distribution functions of AA, AB and CA pairs at different temperatures. For clarity the individual curves have been shifted vertically by 0.1n (n = 1, 2, ...).

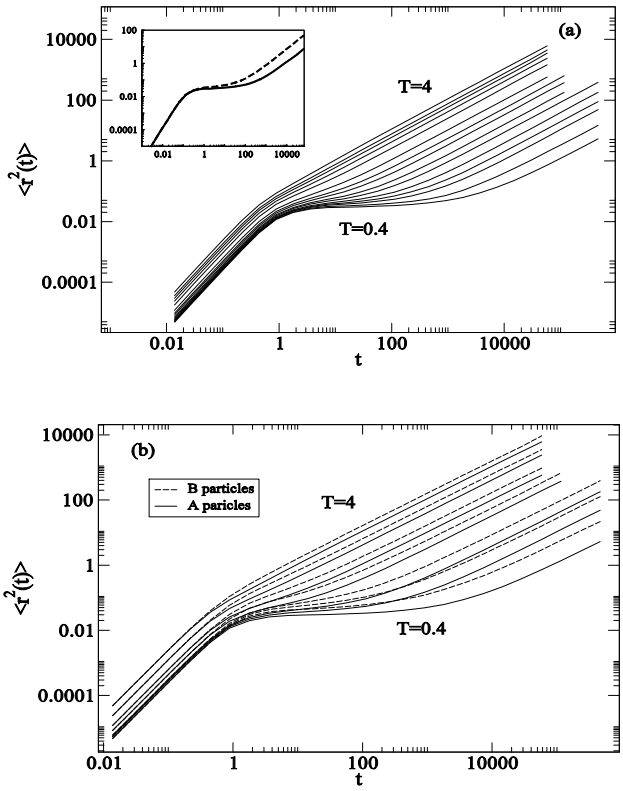

Fig. 2. (a) The logarithmic plot of the mean squared displacement of A particles for the entire temperature range investigated. Inset shows a comparison of the MSDs for bulk BLJ (solid curve) and BLJ+Gold (dashed curve) at a temperature $T = 0.45$. (b) The MSDs of A and B particles are shown at temperatures $T = 4, 2, 1, 0.7, 0.5, 0.45$ and 0.4 for comparison. In the entire temperature range the B particles diffuse faster than the A particles.

particles is about $<r^2> = 0.04$ corresponding to a root-mean-square distance of 0.2, which is significantly smaller than the atomic diameter (that is unity). Within this distance, a tagged particle traps in a cage of its nearest neighbors. The time extension of this plateau enhances upon lowering the temperature. The inset of Fig. 2a demonstrates the MSDs at $T = 0.45$ for both our system of the BLJ+Gold (upper dashed curve) and the bulk BLJ (lower solid curve) for comparison. The β-relaxation regime corresponding to the plateau, is

shorter than that in the bulk BLJ as the gold nanoparticle has influenced the structure of the liquid (by attracting the BLJ particles), and its dynamics as well by providing more free volume for the BLJ particles further away from the nanoparticle to diffuse. Figure 2b shows the MSDs for A and B particles for comparison. The larger A particles diffuse slower than the B particles, and this effect becomes more pronounced with lowering the temperature as the A particles tend to create a layer around the massive nanoparticle. This effect causes the A particles to move even slower, while there will be more space for the diffusion of B particles. The diffusive motion of simple liquids in equilibrium is restored after leaving the plateau. A linear fit to this long-time regime, gives the diffusion constant D according to the Einstein relation $<r^2(t)> = 6Dt$. The results for the diffusion constants in the range of temperatures investigated, are shown in Fig. 3 for A, B and C particles.

A and B particles behave in a similar way, but as the temperature is reduced the ratio of the diffusion coefficients $D(B)/D(A)$ changes from 1.4 at $T = 4$ to 4.15 at $T = 0.4$. The diffusion of C particles at high temperatures can be determined in the same way as the A and B particles (*i.e.* by a linear fit to the long-time regime of the corresponding MSD curve), however, below the onset of slow dynamics $T_{on} \approx 0.7$, it gets harder for the gold nanoparticle to get rid of the adsorbed A particles and to break out of its cage as a result of the high attractive potential and the low temperature. In this regime of temperatures, it is difficult to accurately calculate the diffusion of C particles from the slope of the corresponding MSD curves and the data shown in Fig. 2 for C particles below $T_{on} \approx 0.7$ must be regarded as a rough estimate. Nevertheless, they are shown to give an overall picture of the diffusion of C particles. The main point is that the C particles consistent with the MCT, behave in a similar manner as the A and B particles even at low temperatures. As discussed in section II for temperatures approaching T_C, the MCT predicts that the diffusion constants must have a power-law dependence on temperature. From the temperature dependence of the diffusion coefficients, we can test this prediction of the MCT as given by Eq. (1). In Fig. 3, the fit to the MCT power-law is also shown. Our best estimates of T_C are 0.40(1) for A particles, 0.40(2) for B particles, and 0.40(6) for C particles. This independence of the T_C from the particle

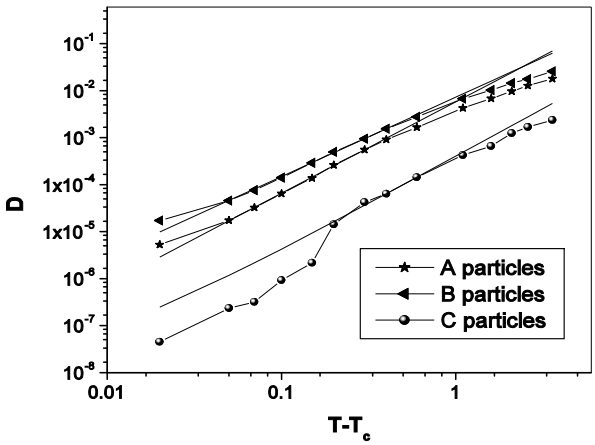

Fig. 3. The diffusion coefficients *vs*. rescaled temperature for A, B and C particles. The straight lines correspond to the MCT fits of Eq. (1). The values of the fit parameters are $T_c = 0.4$ for A, B and C particles and the exponent is 1.94 for A particles, 1.57 for B particles, and 2.02 for C particles.

type, is in excellent agreement with the predictions of MCT. The exponent γ is found to be 1.94(11) for A particles, 1.57(10) for B particles and 2.02(33) for C particles. The range of validity of the MCT in terms of the reduced distance from the apparent dynamic transition point $\varepsilon = (T - T_c)/T_c$ is $0.05 < \varepsilon < 0.75$ corresponding to the temperature range $0.42 < T < 0.7$ used for the straight line fits shown in Fig. 3. The range of validity of the MCT reported for bulk BLJ is much wider: $0.07 < \varepsilon < 1.3$. The deviation from the power-law behavior for temperatures below the lower limit, $T = 0.42$, is accounted for by the cooperative motion or activated hopping that is not included in the ideal form of the MCT.

Dynamics in Wave-Vector Space

As pointed out in section II, in normal liquids the intermediate scattering function has an exponential decay, however in supercooled regime a plateau appears at the intermediate times or the β- relaxation regime. Figure 4 shows the behavior of intermediate scattering function (ISF) for both A (solid line) and B particles (dashed line) at $q_{maxA} = 7.16$ and $q_{maxB} = 5.5$, respectively. On lowering the temperature, a

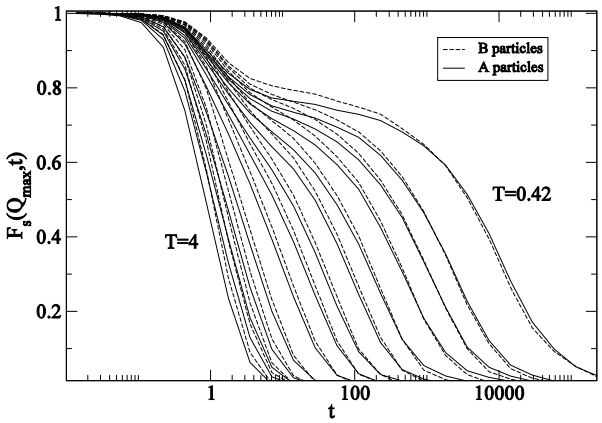

Fig. 4. Intermediate scattering function of A and B particles for whole temperature range investigated. By decreasing temperature a plateau appears and become more pronounced in lower temperature.

small plateau appears and it becomes more pronounced at lower temperatures. A similar behavior was seen in the bulk BLJ. But the presence of nanoparticle causes the length of this plateau to shrink for the reasons explained in discussing the MSDs.

Figures 5a and b include the KWW fit of Eq. (3): the three fit parameters include stretching exponent β, relaxation time τ and the effective non-ergodicity parameter. Still in the presence of gold nanoparticle a remarkable agreement with the data is found.

To test whether the time-temperature superposition is still valid, in Figs. 6a and b we have plotted the ISF as a function of rescaled time with respect to the KWW relaxation time t/τ (T) for both A and B particles, respectively. For times in the late β-relaxation and early α relaxation region, the curves at low temperatures fall onto a master curve. This figure also contains the fitting curves according to von-Schweidler functional form Eq. (5). The values of b exponent are almost the same for both particle types:

$$f_{QA} = 0.789 \quad h_{QA} = 0.54 \quad b = 0.44$$

$$f_{QB} = 0.82 \quad h_{QB} = 0.56 \quad b = 0.445$$

In the bulk the values of b exponent are 0.51 for A particles

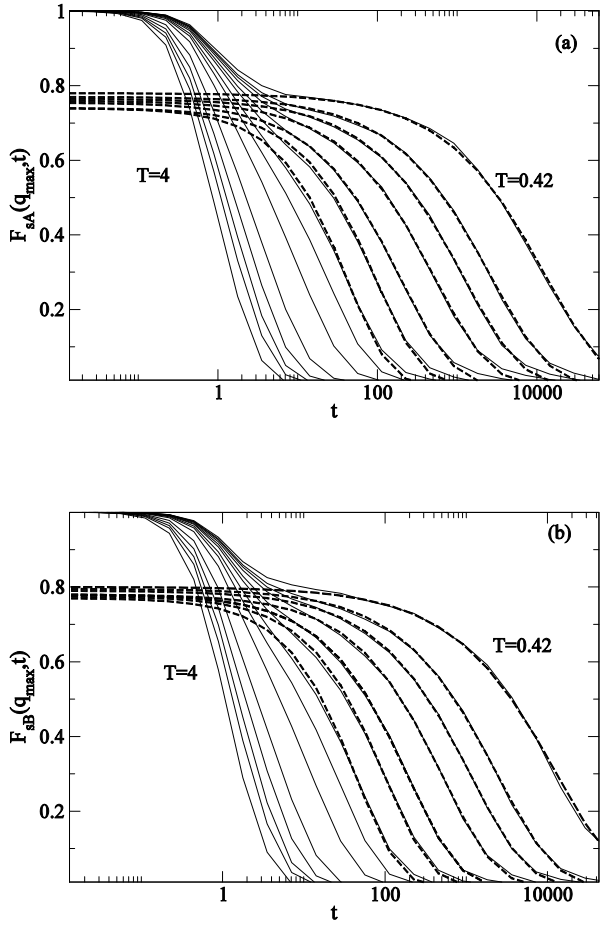

Fig. 5. (a) and (b) show the ISF as a function of t including the KWW fit. For temperatures below the onset temperature a remarkable agreement with KWW equation is found.

and 0.46 for B particles, however, we see that the existence of gold nanoparticle leads to decrease these values.

SUMMARY AND DISCUSSION

With the aid of canonical molecular dynamic simulations, changes of dynamic properties of Kob-Anderson binary Lennard-Jones liquid in the presence of a gold nanoparticle were explored. The investigation of radial distribution functions of the AA, AB and AC pairs, led to similar conclusions as in the bulk BLJ, however, $g_{CA}(r)$ gives

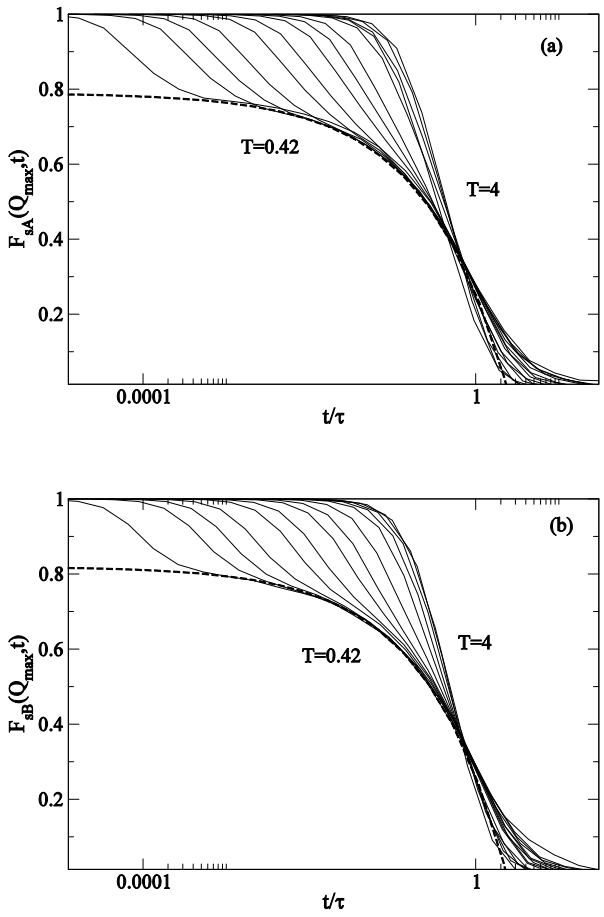

Fig. 6. ISF of Fig. 5 rescaled with respect to the corresponding KWW relaxation time for both A (top panel) and B (bottom panel) particles. The dashed curve represents the von Schweidler fit.

evidence that the A particles create a layer around the nanoparticle. This causes the B particles to move faster than A particles in the entire temperature range by providing more space for the motion of B particles. In the plot of mean squared displacement *vs*. time, we see that in the diffusive regime the slope of the B particles, which is related to the diffusion constant, is larger than that of the A particles. Power-law fits to the diffusion coefficients extracted from the slope of the MSDs, give an estimate of $T_c = 0.4$ for all A, B and C particle types. The exponent γ is 1.94(11) for A particles, 1.57(10) for B particles and 2.02(33) for C particles.

The MCT predicts that the exponent γ is a universal exponent. However, these values for γ are in agreement with those calculated for the bulk BLJ: $\gamma = 2$ and 1.7 for A and B particles, respectively [6]. The MCT crossover temperature *Tc*, is reduced with respect to the bulk BLJ. The *Tc* depression is related to the enhanced dynamics of BLJ particles in the presence of gold nanoparticle that strongly attacts the BLJ particles. Clearly, the structural changes affected by the gold nanoparticle have also enhanced the diffusion of A and B particles in comparison with the bulk BLJ. The range of validity of the MCT in the α-relaxation regime is much limited in comparison with the bulk BLJ. The range of validity in the bulk BLJ is $0.07 < \varepsilon < 1.3$ against $0.05 < \varepsilon < 0.75$ found in our system. Clearly, the existence of gold nanoparticle has changed the structure of the system and as a result of this structural changes the dynamics of the BLJ particles changes, causing to decrease the range of validity of the MCT. A similar effect has been reported in other systems [17]. In wave vector space, intermediate scattering function shows a behavior similar to what MCT predicts. In the late α-relaxation regime, the curves of ISF have stretched exponential form, which obey KWW analytical function. The curves of ISF, when plotted *vs*. rescaled time, show a collapse onto a master curve. This master curve in the early α-relaxation times can be fitted well by von Schweidler analytical function.

REFERENCES

[1] U. Bengtzelius, W. Götze, A. Sjölander, J. Phys. C 17 (1984) 5915.

[2] L. Berthier, Physics 4 (2011) 42.

[3] T. R. Kirkpatrick, D. Thirumalai, P.G. Wolynes, Phys. Rev. A 40 (1989) 1045.

[4] F.H. Stillinger, Science 267 (1995) 1935.

[5] D. Kivelson, G. Tarjus, X. Zhao, S.A. Kivelson, Phys. Rev. E 53 (1996) 751; D. Kivelson, S.A. Kivelson, X. Zhao, Z. Nussinov, G. Tarjus, Physica A 219 (1995) 27.

[6] W. Kob, H.C. Andersen, Phys. Rev. E 51 (1995) 4626; Phys. Rev. E 52 (1995) 4134.

[7] P. Gallo, R. Pellarin, M. Rovere, Phys. Rev. E 67 (2003) 041202; Phys. Rev. E 68 (2003) 061209.

[8] K.V. Sarathy, K.S. Narayan, J. Kim, J.O. White, Chem. Phys. Lett. 318 (2000) 543.
[9] F.W. Starr, T.B. Schrøder, S.C. Glotzer, Phys. Rev. E 64 (2001) 021802.
[10] C. Caronna, Y. Chushkin, A. Madsen, A. Cupane, Phys. Rev. Lett. 100 (2008) 055702.
[11] C. Roberts, T. Cosgrove, R.G. Schmidt, G.V. Gordon, Macromolecules 34 (2001) 538.
[12] M. Kobayashi, Y. Rharbi, L. Brauge, L. Cao, M.A. Winnik, Macromolecules 35 (2002) 7387.
[13] S. Sastry, P.G. Debenedetti, F.H. Stillinger, Nature 393 (1998) 554.
[14] D.R. Richman, P.C. Charbonneau, J. Stat. Mech. (2005) P05013.
[15] Lecture Notes on Slow Relaxations and Nonequilibrium Dynamics in Condensed Matter, Les Houches July 1-25, 2002; Les Houches Session LXXVII; J.L. Barrat, M. Feigelman, J. Kurchan, J. Dalibard (Eds.), Springer, Berlin, 2003, pp. 199-270.
[16] S.P. Das, Rev. Mod. Phys. 76 (2004) 786.
[17] P. Scheilder, W. Kob, K. Binder, Europhys. Lett. 52 (2000) 277; 59 (2002) 701.